Lithos 184–187 (2014) 436–446

Contents lists available at ScienceDirect

Lithos

journal homepage: www.elsevier.com/locate/lithos

Early Permian to Late Triassic batholiths of the Chilean Frontal Cordillera (28°–31°S): SHRIMP U–Pb zircon ages and Lu–Hf and O isotope systematics

Francisco Hervé [a,b,*], C. Mark Fanning [c], Mauricio Calderón [b], Constantino Mpodozis [d]

[a] Escuela de Ciencias de la Tierra, Universidad Nacional Andrés Bello, Salvador Sanfuentes 2375, Santiago, Chile
[b] Departamento de Geología, Universidad de Chile, Plaza Ercilla 803, Santiago, Chile
[c] Research School of Earth Sciences, Australian National University, Canberra, Australia
[d] Antofagasta Minerals, Apoquindo 4001, Santiago, Chile

ARTICLE INFO

Article history:
Received 19 March 2013
Accepted 19 October 2013
Available online 31 October 2013

Keywords:
Elqui–Limarí batholith
Permian
Oxygen and Lu–Hf isotopes
Magma sources

ABSTRACT

One of the major geological units of the Main Andean Range (Frontal Cordillera) of north–central Chile is a group of composite and heterochronous late Paleozoic–early Mesozoic batholiths that extends for 500 km roughly NS along from 26° to 31°S. Ten new SHRIMP zircon crystallization ages together with 11 recently published U–Pb zircon ages by other authors indicate an episodic intrusion history which can be divided in 4 groups: Mississippian (earliest Carboniferous; 330–326 Ma), Cisuralian (earliest Permian; 301–284 Ma), latest Permian to Middle Triassic (264–242 Ma) and Late Triassic (225–215 Ma). Volcanic rocks in the area span a similar time. Lu–Hf and O isotopic systematics in zircon grains from eight of the plutonic rocks indicate the magma source areas have contributed variable amounts of crustal and mantle components. Zircon $\delta^{18}O$ values evolve from crustal values (+7‰) in the earliest Permian intrusives to mantle values in the latest Permian to Upper Triassic, including evidence for likely hydrothermal alteration of the source (+4‰). Zircon εHf values vary in a good linear correlation with the $\delta^{18}O$ isotopes, from −6 to 0 in rocks older than 270 Ma increasing to + 2 to +7 from Lower to Upper Triassic (250 to 215 Ma). The petrogenetic constraints indicated by these values, suggest that the influence of magma sources varied with time from predominantly crustal to mantle like. In accord with the regional tectonic models, the earliest Permian rocks were generated in a subduction-related magmatic arc, which varied towards an extension-related environment in the latest Permian and Triassic.

© 2013 Published by Elsevier B.V.

1. Introduction

Some of the main geological units of the Andean Range of north–central Chile between latitudes 26° and 31°S are the composite Elqui–Limarí, (ELB), Chollay (ChB) and Montosa–El Potro (MPB) batholiths which were assembled during the Carboniferous to Triassic (Fig. 1; Mpodozis and Cornejo, 1988; Mpodozis and Kay, 1992; Mpodozis et al., 1993; Nasi et al., 1985; Pankhurst et al., 1996; Parada, 1988; Parada et al., 1981, 2007). They form part of an extensive belt of Late Paleozoic to early Mesozoic intrusives that extends from central Peru (Cordillera de Marañón; Chew et al., 2007; Miskovic and Schaltegger, 2009) across the Cordillera de Domeyko in northern Chile (26°S; Mpodozis et al., 1993), the Frontal Cordillera in San Juan-Mendoza (32°S), Argentina (Gregori and Benedini, 2013; Gregori et al., 2003), the San Rafael Block in southern Mendoza (34–36°S; Kleiman and Japas, 2009; Rocha-Campos et al., 2011), and the Lihuel–Cahuel region in La Pampa province (Kay et al., 1989; Lambías and Sato, 1990; Llambías and Sato, 1990,1995). These rocks have been considered by Mpodozis and Kay (1992) to have resulted from subduction-related and post-subduction magmatism along the western Gondwana margin during the final stages of Gondwana assembly and the initial stages of Pangea breakup.

According to models presented by Mpodozis and Ramos (1989), the batholiths of the Chilean Frontal Cordillera (28°–31°S) were emplaced into a basement which includes continental rocks (Chilenia Terrane) that were accreted to the western Gondwana margin during the consolidation of the accretionary Terra Australis Orogen (Cawood, 2005). This study aims to establish a well defined geochronological framework for the evolution of the Elqui Limarí and Chollay batholiths, to contribute to an understanding of the nature of the magma sources and to discuss the mechanisms by which mantle, crustal and subducted components are involved in the genesis of magmatic arcs. For these purposes a coupled Hf and O isotope study was carried out on magmatic zircon grains dated by SHRIMP U–Pb analyses.

* Corresponding author at: Departamento de Geología, Universidad de Chile, Plaza Ercilla 803, Santiago, Chile.
E-mail addresses: fherve@cec.uchile.cl, fherve@unab.cl (F. Hervé).

0024-4937/$ – see front matter © 2013 Published by Elsevier B.V.
http://dx.doi.org/10.1016/j.lithos.2013.10.018

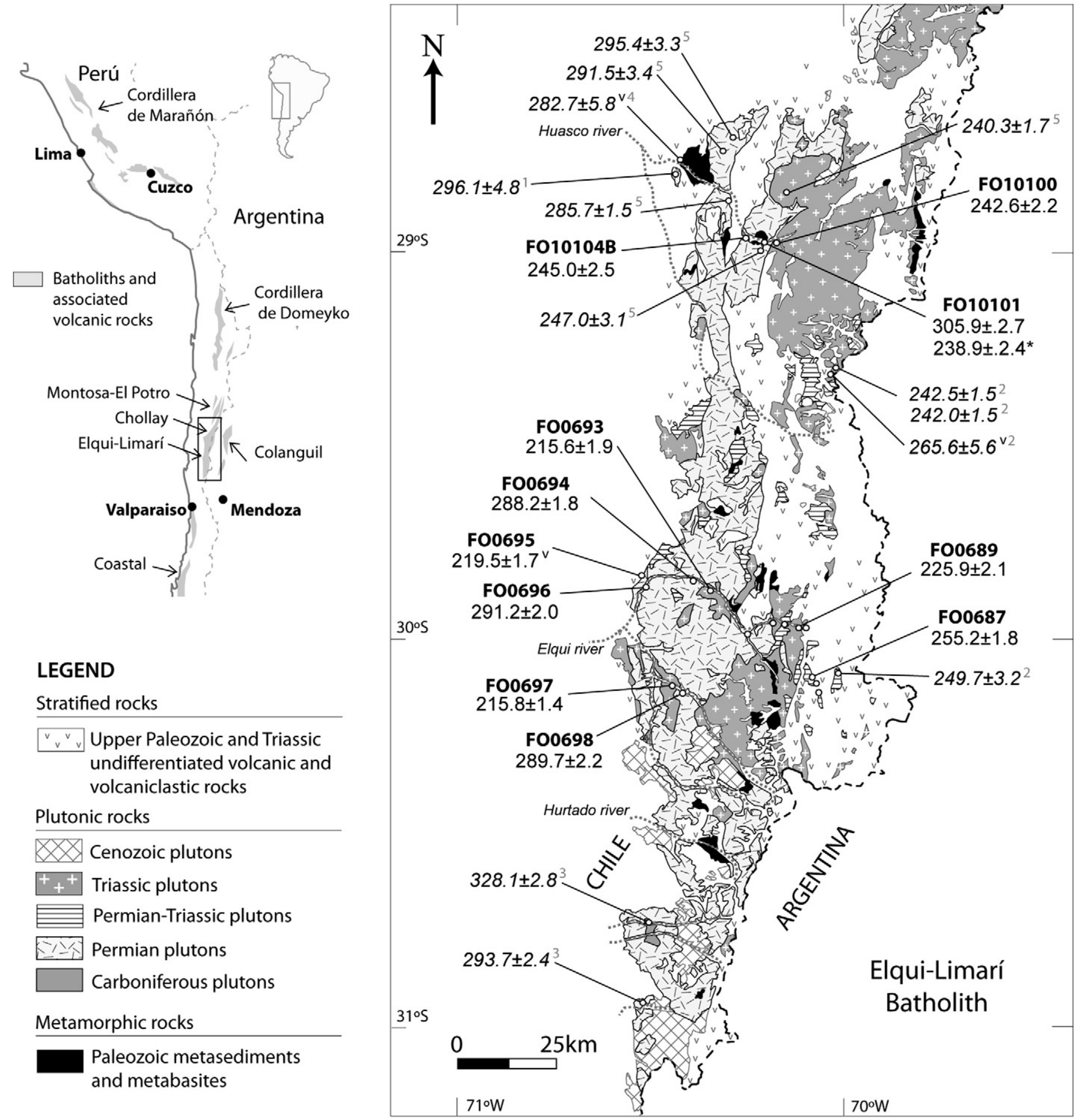

Fig. 1. Geological map which shows the distribution of the Elqui Limari, Chollay and Colanguil batholiths in the high Andes of north-central Chile between 29–31°S (modified from Sernageomin, 2003). The location of the analyzed samples and their U–Pb crystallization ages are indicated. * Indicates ages of metamorphic zircon rims in gneisses. [V] Indicates the volcanic origin of studied rocks. Additional age data, in italics, are previously published U–Pb zircon crystallization ages (1, Pankhurst et al., 1996; 2, Martin et al., 1999; 3, Pineda and Calderón, 2008; 4, Salazar et al., 2009; 5, Coloma et al., 2012). Dashed line-work represents main rivers.

2. Geological setting and plutonic stratigraphy of the Elqui–Limarí and Chollay batholiths

The Elqui–Limarí and Chollay Batholiths are well exposed along the upstream subsidiaries of the Huasco (29°S), Elqui (30°S) and Limarí (31°S) river valleys (Fig. 1). Host rocks include, in the northern Huasco Valley region, small roof pendants of gneisses (La Pampa Gneisses; Álvarez et al., 2013; Ribba et al., 1988) and larger outcrops of psammitic and pelitic schists, limestones and metabasites (El Tránsito Metamorphic Complex). The protoliths of these rocks formed after 380 Ma and they were metamorphosed before 300 Ma (Álvarez et al., 2011; Reutter, 1974; Ribba et al., 1988). The batholiths also intrude slightly metamorphosed sedimentary sequences of meta-greywackes and shales of supposed ?Devonian to Carboniferous age, such as the Las Placetas Formation in the Huasco region (Nasi et al., 1990; Reutter, 1974) and El Cepo Complex and Hurtado formations in the Elqui–

Limarí region (Mpodozis and Cornejo, 1988). Both batholiths are unconformably overlain by Late Triassic siliceous volcanic rocks (Elqui Valley) and Jurassic shallow marine limestones and sandstones (Lautaro and Tres Cruces formations) that accumulated in a back-arc setting (Mpodozis and Cornejo, 1988).

The Rb–Sr and K–Ar ages reported by Parada et al. (1981), Mpodozis and Cornejo (1988), Nasi et al. (1990) and Mpodozis and Kay (1990, 1992) indicated that pluton emplacement in the Elqui–Limarí, Chollay, and Montosa–El Potro batholiths took place between 330 and 200 Ma. The three batholiths are composed of a large number of plutons, exhibiting sharp mutual contacts between individual intrusive bodies and the host rocks. The plutons vary in composition from coarse-grained biotite-hornblende tonalite and granodiorite to two mica granodiorite and leucocratic pink biotite granite, subvolcanic rhyolitic porphyry intrusions, and small gabbro stocks. Nasi et al. (1985, 1990) and Mpodozis and Cornejo (1988) who followed the nomenclature system applied by Pitcher et al. (1985) to the Cretaceous Peruvian Coastal Batholith, originally grouped the different plutons within two "superunits" (later described as plutonic complexes by Mpodozis and Kay, 1992) comprising plutons depicting similar field relations, petrography, and broadly similar ages. The older Elqui Complex, originally attributed to the Carboniferous–early Permian includes four second-order plutonic units: Guanta (biotite–hornblende tonalites), Montosa (biotite granodiorites), Cochiguás (biotite–muscovite granodiorites and granites) and El Volcán (cataclastic biotite granites and granodiorites). The second and assumed younger, (Permian to Triassic) Ingaguás Complex, largely comprises much more felsic plutons grouped in 4 plutonic units: Los Carricitos (biotite–hornblende granodiorites), Chollay (coarse grained monzogranites), El León, (medium grained, pink, biotite granites) and Colorado ("red" rhyolitic porphyries and graphic granites) grouped together with minor gabbro stocks. The emplacement of the Ingaguás Complex was thought to occur synchronously with the eruption of large volumes of volcanic rocks (Pastos Blancos Formation) that were correlated with the "Permo-Triassic" Choiyoi Group of the Argentine Frontal Cordillera (Choiyoi Large Igneous Province; Kay et al., 1989)

Mpodozis and Kay (1990, 1992) proposed that the Elqui Complex was the product of subduction-related magmatism that took place on the Gondwana margin after the collision of the Chilenia terrane in the Devonian (Ramos et al., 1986). In contrast, the younger Ingaguás complex was considered to have been generated during a pause in subduction after the San Rafael orogenic phase, when extensional conditions prevailed along the Gondwana margin (Lambías and Sato, 1990; Mpodozis and Kay, 1990, 1992). In recent years, new zircon U–Pb ages (e.g. Álvarez et al., 2013; Coloma et al., 2012; Martin et al., 1999; Pankhurst et al., 1996; Pineda and Calderón, 2008; Salazar et al., 2009) have, however, began to challenge the original definitions and the model of the batholiths as previously proposed (see above), In this contribution, we present new U–Pb SHRIMP zircon crystallization ages for the ELB and ChB together with data on the O and Lu–Hf isotopic compositions of a representative number of the dated zircons. This information constrains the age span of the batholith assembly, and enables us to monitor changes with time in the characteristics of the source areas of the magmas that gave rise to the batholiths. A comparison with other Late Paleozoic batholiths in Chile and Argentina is made.

3. Analytical methods

Zircons were handpicked from heavy mineral concentrates obtained by the standard methods of crushing, grinding, Wilfley table, magnetic and heavy liquid separation at Universidad de Chile. Zircon analyses were carried out at RSES (Research School of Earth Sciences, The Australian National University, Canberra). The grains were mounted in epoxy, sectioned approximately in half and polished, and CL (cathodoluminescence) images were obtained for every zircon. U–Th–Pb analyses were made using the sensitive high-resolution ion microprobes (SHRIMP II and SHRIMP RG) following the procedures described by Williams (1998). Between 15 to 20 grains were analyzed in each sample to characterize well the age variation present. Weighted mean $^{206}Pb/^{238}U$ ages are reported with a 2 sigma uncertainty.

Oxygen ($^{18}O/^{16}O$) and Lu–Hf ($^{176}Lu/^{177}Hf$ and $^{176}Hf/^{177}Hf$) isotope ratios were measured for a selection of zircon grains with the aim to characterize the isotopic composition of the magmas from which they crystallized, and thereby investigate the nature of the source(s) of these magmas. Following the U–Pb analyses, the SHRIMP U–Pb pits, 1–2 μm deep, were lightly polished away and oxygen isotope analyses were made in exactly the same location using SHRIMP II fitted with a Cs ion source and an electron gun for charge compensation as described by Ickert et al. (2008). Oxygen isotope ratios were determined in multiple-collector mode using an axial continuous electron multiplier (CEM) triplet collector, and two floating heads with interchangeable CEM — Faraday Cups. The Temora 2, Temora 3 and FC1 reference zircons were analyzed to monitor and correct for isotope fractionation. The measured $^{18}O/^{16}O$ ratios and calculated $\delta^{18}O$ values have been normalized relative to an FC1 weighted mean $\delta^{18}O$ value of 5.4‰ (Ickert et al., 2008). Reproducibility in the Duluth Gabbro FC1 reference zircon $\delta^{18}O$ value ranged from ± 0.23‰ to 0.47‰ (2σ uncertainty) for the analytical sessions, with most of the reference zircon analytical uncertainties in the range 0.21–0.42‰ (±2σ). As a secondary reference material, zircons from the Temora 2 or Temora 3 zircons analyzed in the same analytical sessions gave $\delta^{18}O$ values of 8.2‰ and 7.59‰ respectively, in agreement with data reported by Ickert et al. (2008, Temora 2: 8.2‰) and Valley et al., unpublished data obtained by the laser fluorination technique for Temora 3 (7.58‰; as reported in Iizuka et al., 2013)

Lu–Hf isotopic measurements were carried out by laser ablation multi-collector inductively coupled plasma mass spectroscopy (LA-MC-ICPMS) using a Neptune MC-ICPMS coupled with a 193 nm HelEx ArF Excimer laser; similar to procedures described in Munizaga et al. (2008). Laser ablation analyses were centered on the same locations within single zircon grains used for both the U–Pb and oxygen isotope analyses described above. For all analyses of unknowns or secondary standards, the laser spot size was *ca.* 47 μm in diameter. The mass spectrometer was first tuned to optimal sensitivity using a large grain of zircon from the Mud Tank carbonatite (see Woodhead and Hergt, 2005). Isotopic masses were measured simultaneously in static-collection mode. A gas blank was acquired at regular intervals throughout the analytical session (every 12 analyses). The laser was pulsed at a 5–8 Hz repetition rate providing an energy density on the sample surface of 3.2–3.6 J/cm^2. Data were acquired for 100 s, but in many cases we selected an interval over which the $^{176}Hf^{177}Hf$ ratios were consistent. Throughout the analytical session several widely used reference zircons (91500, FC-1, Mud Tank and Temora 2 or 3) were analyzed to monitor data quality and reproducibility. Signal intensity was typically ca. 5–6 V for total Hf at the beginning of ablation, and decreased over the acquisition time to 2 V or less. Isobaric interferences of ^{176}Lu and ^{176}Yb on the ^{176}Hf signal were corrected by monitoring the signal intensities of ^{175}Lu and ^{173}Yb, ^{172}Yb and ^{171}Yb. The calculation of the signal intensity for ^{176}Hf also involved independent mass bias corrections for Lu and Yb.

4. Samples

Seven of the analyzed samples belong to the ELB and one is a volcanic sample from the Triassic Las Breas Formation which overlies the western edge of the ELB in the Elqui valley region. Additionally we have analyzed one sample of the La Pampa Gneisses which is intruded by the Chollay batholith in the Huasco river section, a sample from the Chollay Batholith and one sample of a mylonitic belt (El Portillo Mylonites). Brief rock descriptions are given in Annex 1, together with an indication of the name of the sampled pluton and its associated intrusive unit as defined by Nasi et al. (1985) and its locality. The new U–Pb SHRIMP ages shown in Table 1 and are also included in Fig. 1.

Table 1
Summary of U–Pb zircon ages.

Sample number and geographical coordinates	Rock type	Unit and locality	Age (Ma)	Error
FO0696 29°51′42″S 70°30′21.2″W	Hornbende–biotite granodiorite	ESU Chapilca pluton	291.2	2
FO0698 30°08′07.5″S 70°24′38.8″W	Biotite–muscovite granite	ESU Cochiguaz unit	289.7	2.2
FO0694 29°50′46.0″S 70°22′59.9″W	Hornbende–biotite tonalite	ESU Guanta unit	288.2	1.8
FO0687 30°05′37.2″S 70°04′31.9″W	Clinopyroxene gabbro	ISU La Laguna gabbro	255.2	1.8
FO0689 29°58′05.8″S 70°06′37.7″W	Porphyritic granite	ISU El Leon Unit	225.9	2.1
FO0697 30°07′01.7″S 70°26′11.4″W	Biotite granite	ISU El Leon Unit Montegrande pluton	215.8	1.4
FO0693 29.8714ºS 70.3391ºW	Megacrystic cordierite–muscovite granodiorite	ISU Los Tilos pluton	215.6	1.9
FO0695 29°49′54.3″S 70°30′38.7″W	Dacite breccia	Las Breas formation Quebrada El Calvario	219.5	1.7
FO10104B 28°57′46.4″S 70°14′51.7″W	Biotite leucogranite	El Portillo mylonites	245.0	2.3
FO10100 28°58′27.5″S 70°10′05.8″W	Leucogranite	Chollay batholith	242.6	2.2
FO10101 28°58′25.8″S 70°11′59.1″W	Cordierite–sillimanite gneiss	Pampa Gneiss	238.9 305.9	2.4* 2.7

Note: Representative CL images of the zircon grains is given in Fig. S1 of the Electronic annex. More detailed comments on the zircons and the U–Pb data and interpretation in Annex 2.

5. Results

5.1. Zircon SHRIMP U–Pb ages

A summary of the new SHRIMP U–Pb zircon age determinations are given in Table 1. Analytical data can be found in Tables S1 to S11 of the Electronic annex. Descriptions of analyzed zircons and interpretations are given in Annex 2. Representative CL images of zircons can be found in Fig. S1 of the Electronic annex. All the obtained ages, with the exception of sample FO11101 (La Pampa Gneisses) can be confidently interpreted as igneous crystallization ages. After the International Stratigraphic Chart of the International Commission on Stratigraphy (IUGS, 2013), all the obtained ages are Permian or Triassic. Tera and Wasserburg concordia plots and age vs. probability diagrams are shown in Figs. 2–6.

5.2. Zircon Lu–Hf and O isotopes

The results of the isotopic analyses are given in Table S12 of the Electronic Annex, and are plotted on Fig. 7. In the εHf vs age diagram (Fig. 7A), it can be seen that the εHf values vary in a general linear fashion from negative values for the zircon grains older than 265 Ma (−5 to 0), to positive values for the Late Permian zircon grains (255 to 265 Ma, 0 to + 4), and increasingly positive for the Late Triassic grains (0 to + 9). This indicates an increasing mantle influence in the magmas with time. In the younger group, only the cordierite-bearing Los Tilos granite has relatively low values (0 to +3) which is likely a consequence of local crustal influences.

On the $\delta^{18}O$ vs age diagram (Fig. 7B) it can be seen that the zircons older than 260 Ma have elevated $\delta^{18}O$ values (average $\delta^{18}O$: 6.4‰). The zircons from Gabbro de la Laguna (255 Ma) have values equivalent to those for Mantle zircon (average 5.2‰) and those from Juntas del Toro pluton (230 Ma) have the lowest value, lower than those for Mantle zircon (average 4.2‰). This suggests that there has been hydrothermal alteration of the source area from which the magma was derived. About half of the zircon grains from the Late Triassic dacitic pyroclastic breccia, the Las Breas Formation (220 Ma) also record very low $\delta^{18}O$ values. Other Triassic samples record either Mantle zircon $\delta^{18}O$ values, or, as in the case of the youngest Los Tilos (215.6 ± 1.9 Ma) cordierite megacrystic granite (average 6.4) the $\delta^{18}O$ values are elevated, close to those recorded by the Early Permian samples. This latter increase in $\delta^{18}O$ values is likely a consequence of locally derived crustal melting.

On an εHf vs $\delta^{18}O$ plot (Fig. 7C) a simple negative linear correlation is defined, ranging from the generally older samples with more negative εHf and elevated $\delta^{18}O$ values (i.e. more crustally derived) to those samples that have more positive εHf and lower $\delta^{18}O$ (i.e. more Mantle-like signatures). There is no marked discontinuity within the entire data set, the Early Permian rocks and the youngest Late Triassic cordierite bearing granodiorite being similar.

6. Discussion

6.1. Host rocks and igneous stratigraphy

Ramos et al. (1986) and Mpodozis and Ramos (1989) proposed that the Elqui–Limarí and Chollay batholiths that were emplaced into the “continental” basement of the Chilenia terrane, supposedly accreted to the South American Gondwana margin during the Devonian (Massonne and Calderón, 2008; Ramos et al., 1986; Willner et al., 2011). One of the few outcrops considered as a possible remnant of that Chilenia basement are La Pampa Gneisses, that form a km-sized gneissic block within the Chollay Batholith in the Huasco river valley (Fig. 1). These rocks were assumed to be part of the Chilenia basement on the basis of a ca.450 Ma Rb–Sr whole rock errorchron published by Ribba et al. (1988). The SHRIMP U–Pb data obtained from sample

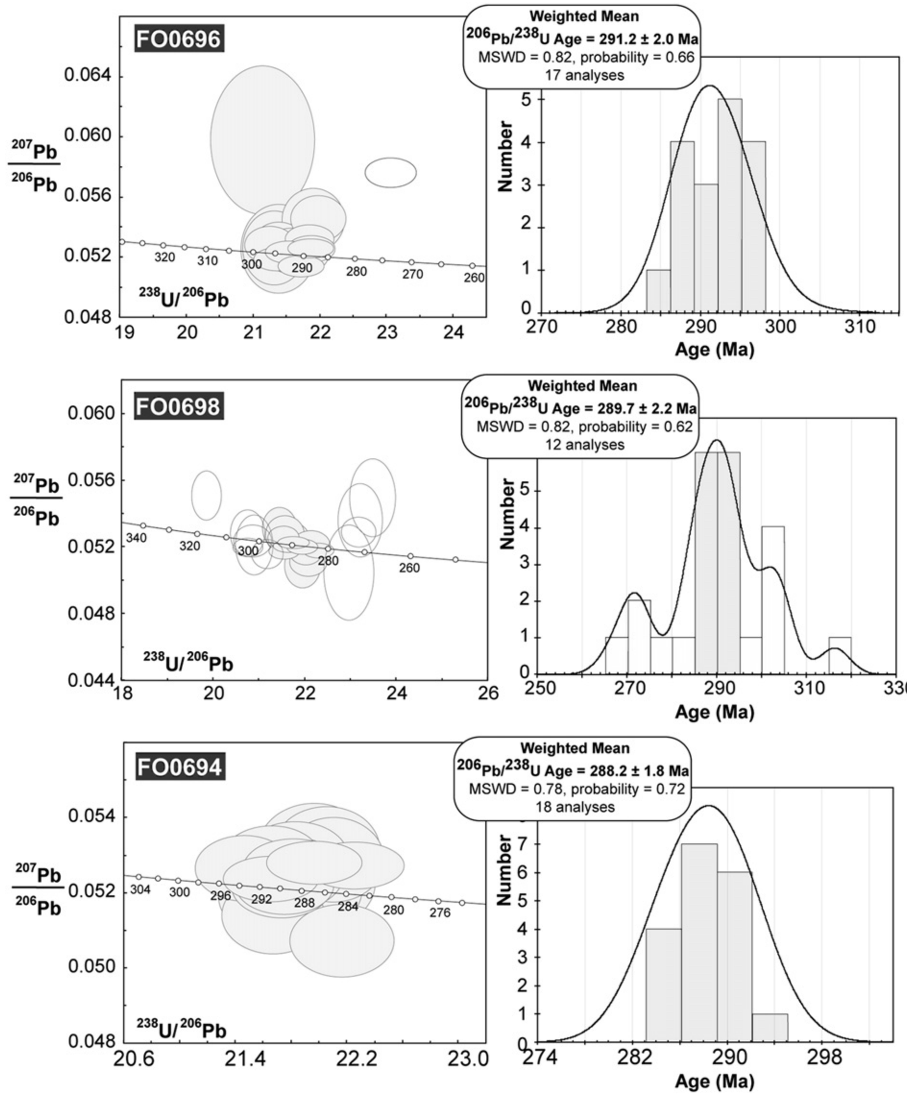

Fig. 2. Tera Wasserburg concordia and age probability density plots for analyzed samples belonging to the Early Permian. FO0696, Hornbende-biotite Granodiorite; FO0698, Biotite–muscovite granite; FO0694, Hornbende-biotite tonalite.

FO10101 (Fig. 6) show that in this sample metamorphic zircon rims of *ca*. 240 Ma grew on igneous zircon cores of ca. 300 Ma. These data are consistent with the U–Pb data reported by Álvarez et al. (2013) showing that the La Pampa Gneisses can no longer be considered as part of the Chilenia basement as the age of the protolith is clearly younger than the age of the inferred collision between Chilenia and Gondwana. The zircon age spectra (Fig. 6) indicate that the protolith was either a Carboniferous metasediment or an anatectic granitoid, and that it was metamorphosed near the Lower Triassic. The age of the granite intruding the neighboring Portillo mylonite is 245 Ma and this age is likely associated with a tectonothermal event in the area. Folded leucogranites within the mylonites testify to high-temperature deformation during the last stages of mylonitization of the host medium-grained tonalitic rocks (Murillo et al., 2012; Ribba et al., 1988).

The map in Fig. 1 includes all the published U–Pb ages for the Elqui–Limarí and Chollay batholiths and equivalent volcanic units plus the new ages presented in Table 1. These data indicate that the region has a protracted magmatic history that lasted more than 110 Ma. In a summary plot of all age data (Fig. 8), four age groups are discernible: A: Mississippian (330–326 Ma, $n = 1$); B: Cisuralian (earliest Permian; 301–284 Ma, $n = 7$); C: latest Permian to Middle Triassic (264–242 Ma, $n = 8$); and D: Upper Triassic (225–215 Ma, $n = 4$). The single age that defines the oldest group might correspond to some of the scattered Early Carboniferous A-type granite plutons, which were intruded in a dominantly extensional setting (Dahlquist et al., 2013). Most of the ages from the two older groups were obtained from plutons originally mapped by Nasi et al. (1985) as part of the Elqui Complex. Nevertheless, and contrary to what Nasi et al. (1985) and Mpodozis and Kay (1992) suggested, the oldest intrusives are not the hornblende-biotite tonalites (Guanta Unit, 296 to 280 Ma) but muscovite-bearing granodiorites (ca. 328 Ma). Two mica granitoids were also emplaced in the Early Permian (289 and 287 Ma) and in the Triassic (242 Ma; Fig. 8) showing that muscovite bearing intrusives were not confined to a single discrete magmatic episode. The new U–Pb data show that the igneous stratigraphy of the Elqui–Limarí and Chollay batholith as originally proposed by Nasi et al. (1985) and Mpodozis and Kay (1990, 1992) needs to be reassessed. Similar dating needs to be carried out for volcanic units considered to be in part age equivalent to the batholiths. Salazar et al. (2009) and Coloma et al. (2012) have highlighted the fact that rhyolitic volcanism spatially linked to the outcrops of the batholith began as early as 300 Ma in the Huasco Valley region near the western border of the Elqui–Limarí Batholith. Also Martin et al. (1999; K–Ar, K–Ar and U–Pb data) showed that the Pastos Blancos Formation cropping out to the east of the ELB and ChB includes two volcanic units that seem to have been emplaced essentially during the Permian (Guanaco Sonso sequence) and the Mid Triassic–Early Jurassic (Los Tilos sequence).

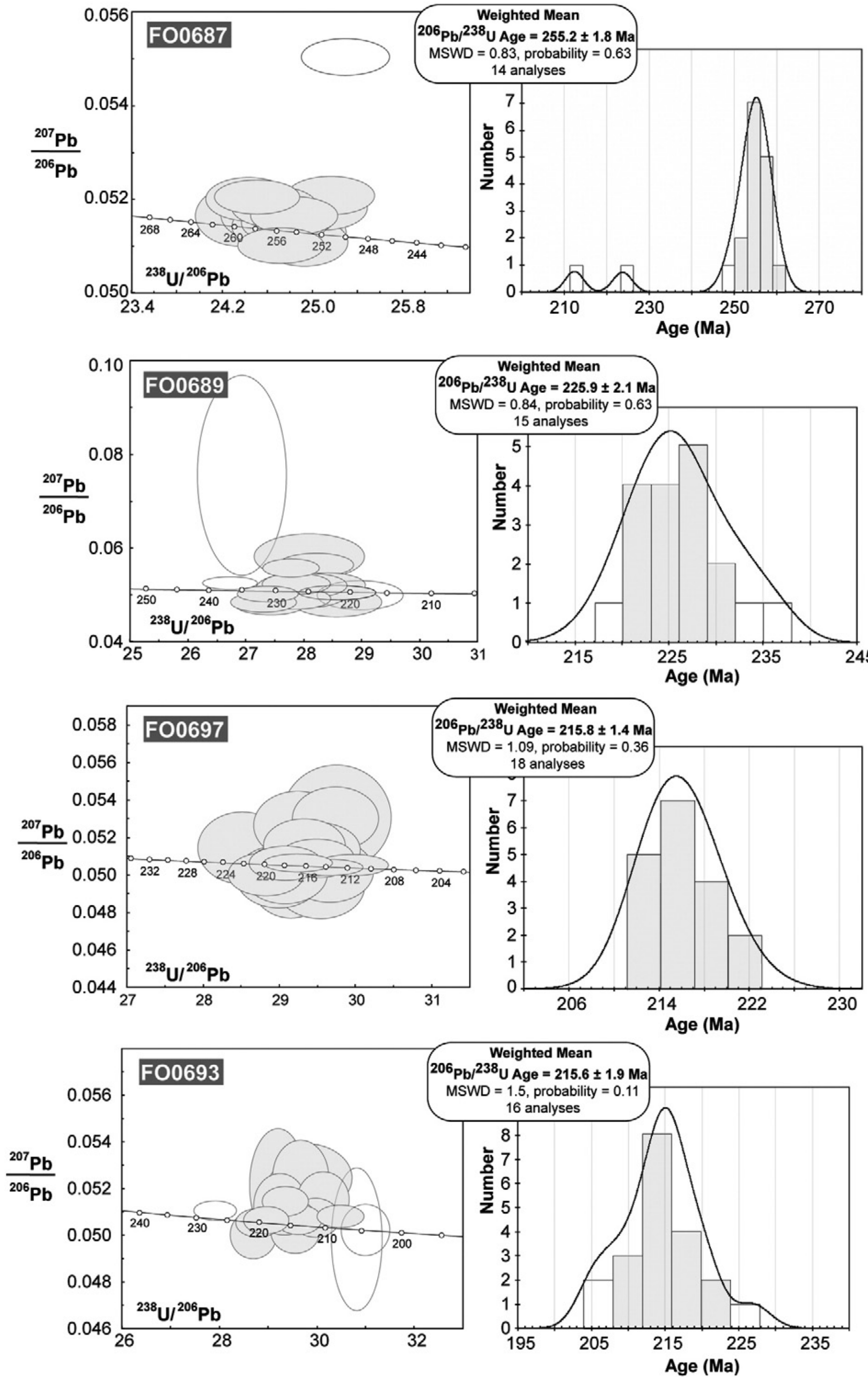

Fig. 3. Tera Wasserburg concordia and age probability density plots for analyzed samples belonging to the Late Permian and Triassic. FO0687, Clinopyroxene Gabbro; FO0689, Porphyritic granite; FO0697, Biotite granite; FO0693, Cordierite–muscovite granodiorite.

Another geochronological result of interest is the age of the dacitic volcanic breccia (FO0695, 219.5 ± 1.7 Ma) collected near the base of the Las Breas Formation, which overlies in stratigraphic contact the Chapilca pluton (291.2 ± 2.7 Ma). These and other field relationships show that the older components of the Elqui–Limarí Batholith were exhumed and uplifted before emplacement of some of the youngest Late Triassic intrusives, such as the Montegrande (215.8 ± 1.4 Ma) and Los Tilos (215.6 ± 1.9 Ma) plutons, which intrude the older, early Permian (301–284 Ma) plutons of the batholith. The age of exhumation can be further constrained by the stratigraphic relationships observed in the Huasco Valley region where fossiliferous Anisian (245–237 Ma) marine sedimentary strata (San Felix Formation; Reutter, 1974; Ribba et al., 1988) overlie metamorphic rocks intruded by early Permian tonalites dated at 296 Ma and 291 Ma (Coloma et al., 2012; U–Pb zircon). Mpodozis and Kay (1992) proposed that the uplift/exhumation of the older component of the ELB was the result of a major deformation event during the mid-Permian which they correlate with the San Rafael Orogenic phase (Lambías and Sato, 1990) recognized in the Argentine Frontal Cordillera and the San Rafael block (López Gamundi, 2006; Rocha-Campos et al., 2011). Compressional conditions for the San Rafael orogenic phase at the Frontal Cordillera near Mendoza City, are bracketed between ca. 284 Ma and 276 Ma. This was followed by an extensional

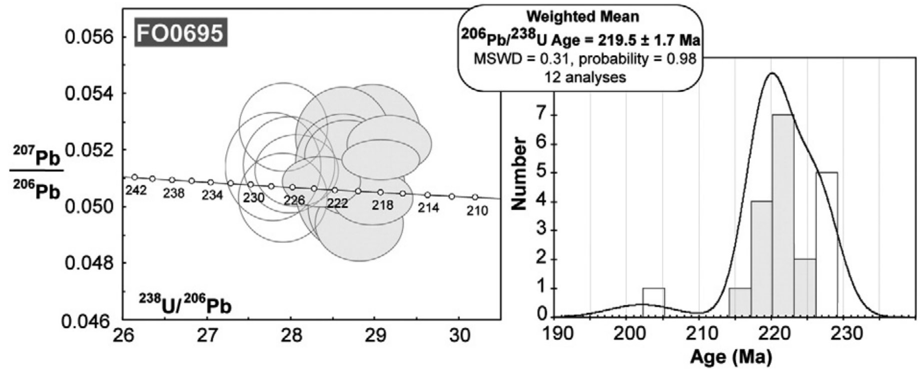

Fig. 4. Tera Wasserburg concordia and age probability density plots for dacite breccia from the Las Breas Formation.

phase that extended into the Triassic (Gregori and Benedini, 2013). It is likely that the Cisuralian magmatic activity in the ELB (Group B; 301–284 Ma) occurred shortly before the San Rafael compressional phase, which in itself is probably diachronic (Fig. 8).

6.2. Magma source: Implications of the O and Hf isotopic data

As shown in Fig. 7, the Late Permian to Triassic intrusives (Groups C and D) and the volcanic breccia from the Triassic Las Breas Formation have zircons with more juvenile isotopic compositions than the Early Permian tonalites and granites of the Early Permian suite (ca. 286–294 Ma). Despite their fractionated chemical character, all samples with Early Permian age record zircon Hf–O isotope compositions pointing to an inherited composition from a "deep" source of magmas, which was not affected by significant assimilation processes during magma ascent through the crust and final pluton emplacement. However, the Hf and O isotopes reveal the presence of a supracrustal component that was acquired at depth in the subcontinental mantle source region of the magmas. By contrast, the Late Permian La Laguna gabbro (ca. 255 Ma) shows zircon Hf–O isotopic compositions indicating mantle derivation, with no ingestion of supracrustal material as indicated by restricted $\delta^{18}O$ ratios between 4.8 and 5.8‰. The zircon Hf ratios indicate the involvement of less radiogenic material in the source, compared to that in the source of the Early Permian suite. The same general characteristics are found in the zircon Hf–O isotope composition of Early and Late Triassic rocks which however, show a wide range of isotopic signatures that can be related to subtle differences in the mantle source of magmas and/or to magmatic processes in crustal reservoirs. The microperthitic biotite leucogranite sample (ca. 226 Ma), with positive mantle-like εHf values, is characterized by low $\delta^{18}O$ ratios (between 3 and 5‰). Hypothetically, this signature can be related to a subcontinental mantle source of magmas metasomatized with variable amounts of fluids or melts derived from high-temperature altered oceanic crust; or to the interaction with high-temperature altered rocks in upper crustal magma chambers (cf. Bolhar et al., 2008). Zircons in the perthitic leucogranite sample (ca. 216 Ma) show similar and slightly enriched Hf–O isotopic ratios to those obtained in La Laguna gabbro, also indicating their derivation from magmas equilibrated with "normal" mantle reservoirs ($\delta^{18}O$ between 4.8 and 5.8‰). The zircons in the biotite–cordierite granodiorite (ca. 216 Ma) show slightly enriched O and Hf

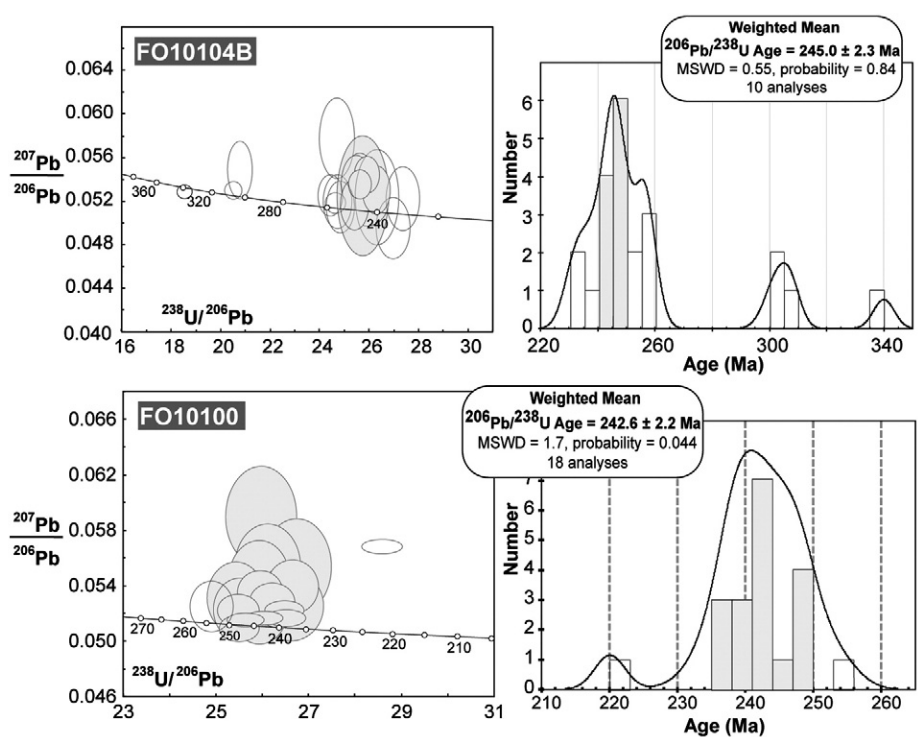

Fig. 5. Tera Wasserburg concordia and age probability density plots for plutonic rocks of the Chollay batholith. FO10104B, Biotite Leucogranite within El Portillo Mylonites; FO10100, Leucogranite.

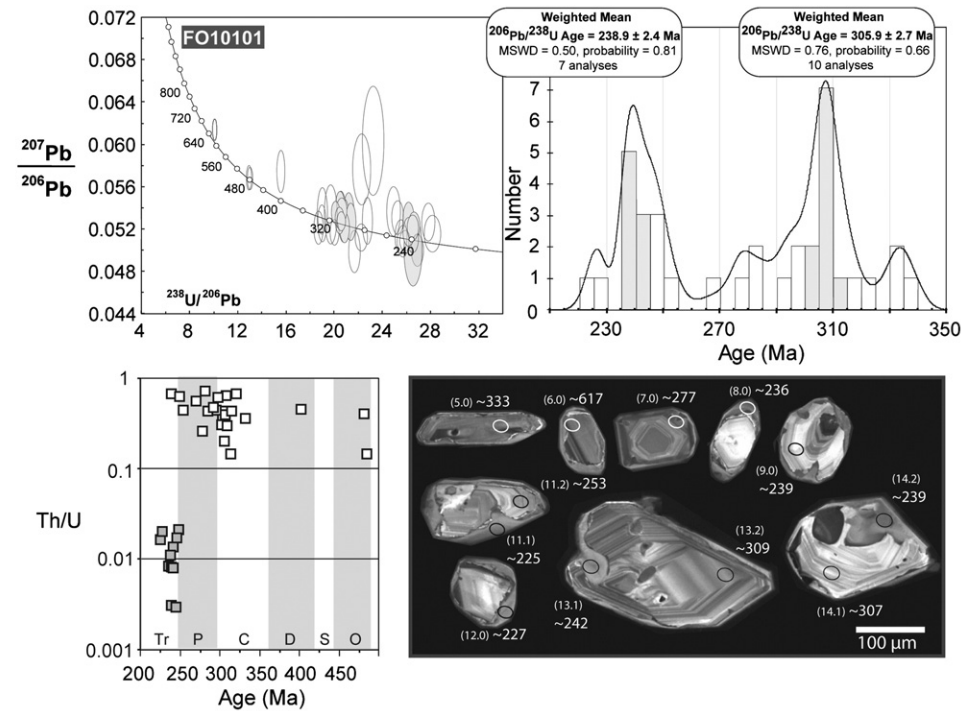

Fig. 6. (a) Tera Wasserburg concordia and age probability density plots for the cordierite–sillimanite gneiss known as La Pampa Gneiss. (b) Th/U vs age diagram for the zircon crystals in which most of Triassic metamorphic rim zircons differ completely from the older core igneous zircons. (c) Cathodoluminiscence images of analyzed zircons.

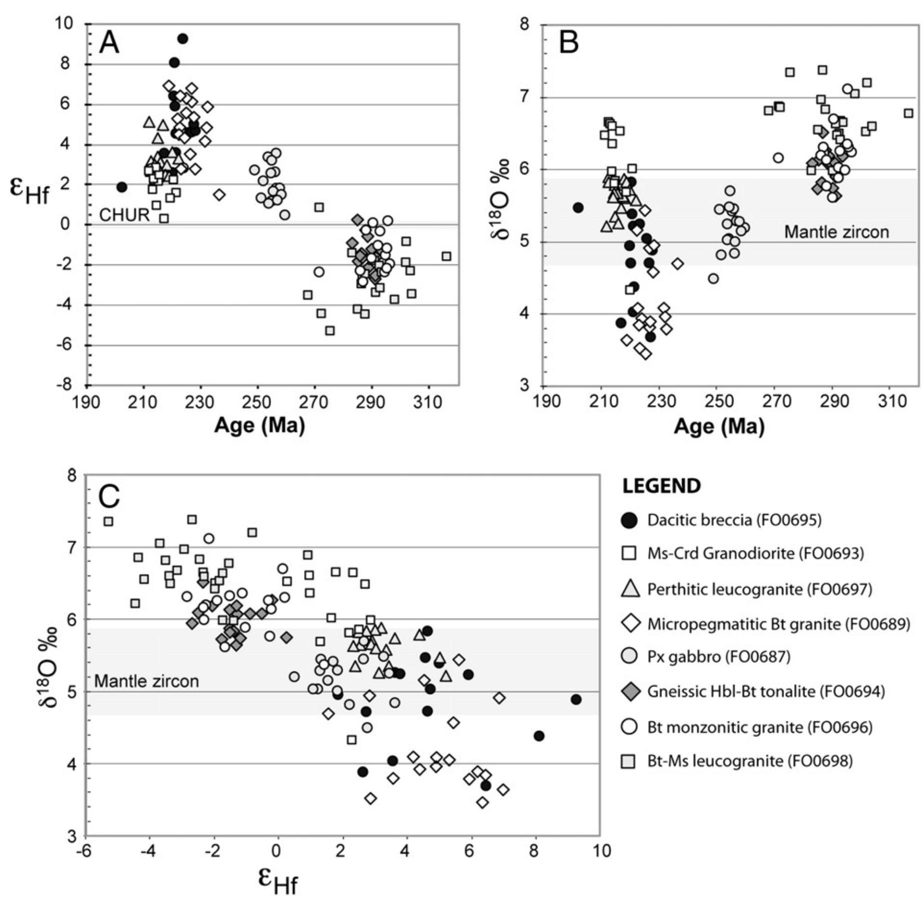

Fig. 7. (A) Initial εHf vs U–Pb zircon age plot. (B) $\delta^{18}O$ vs U–Pb zircon age plot. (C) Initial εHf vs $\delta^{18}O$ plot. The mantle zircon $\delta^{18}O$ values (5.3 ± 0.6‰ (2σ)) are from Valley et al. (2005).

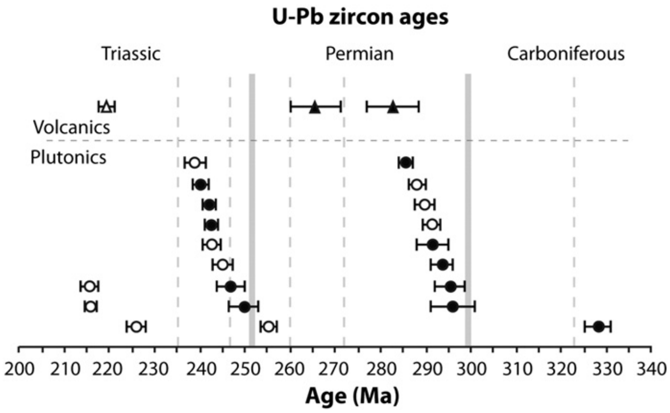

Fig. 8. Age diagram showing the distribution of U–Pb zircon ages in the Elqui–Limarí and Chollay batholiths. Black circles and triangles: data from Pankhurst et al. (1996), Martin et al. (1999), Pineda and Calderón (2008), Salazar et al. (2009), Coloma et al. (2012). Open circles and triangle: this paper.

ratios compared those in the coeval perthitic leucogranite, indicating the involvement of more radiogenic suprascrustal material. Finally, the zircons from the volcanic breccia (ca. 219 Ma) show a diversity of εHf and $\delta^{18}O$ values indicating their formation at different stages of the evolving magmatic reservoirs, probably subjected to injection of mafic magmas and partial isotopic homogenization.

6.3. Late Paleozoic tectonics and the frontal Cordillera batholiths

Mpodozis and Kay (1992) suggested that the Chilean Frontal Cordillera batholiths were formed as result of subduction processes along the Pacific margin of Gondwana after the collision and suture of the Chilenia Terrane at around 390 Ma. This new arc magmatism was preceded by the emplacement of a suite of Mississippian plutons with U–Pb ages ranging from 350 to 340 Ma (Astini et al., 2009; Alasino et al., 2012; Dahlquist et al., 2013; Grosse et al., 2009; Martina et al., 2011) that is widely distributed across the Sierras Pampeanas of Western Argentina and shows A-type to within plate geochemical signatures. These have been considered by Astini et al. (2009) to be post-collisional intrusives, emplaced under extensional conditions that prevailed after the collision of Chilenia collision, and before a new arc was established over the former Chilenia microplate. The early Permian metaluminous Guanta-type calc alkaline tonalites of the Elqui–Limarí Batholith were interpreted by Mpodozis and Kay (1992) as the roots the late Carboniferous–early Permian arc. Peraluminosus biotite–muscovite granitoids such as those from the Chapilca and Cochiguás plutons, were explained as being derived from magmas syntectonically emplaced later into thickened crust during the San Rafael event.

Our new U–Pb data, however, do not fit with that model, as the Chapilca and Cochiguás intrusives are essentially contemporaneous with the Guanta pluton tonalite. Various authors (Bahlburg and Hervé, 1997; Bahlburg et al., 2009; Mpodozis and Ramos, 1989; Willner et al., 2011) agree that during the Devonian, the outboard Pacific margin Gondwana was passive, supporting a thick sedimentary wedge. Under these conditions an alternative view to explain the strong upper crustal signatures observed in the peraluminous early Permian plutons is that they reflect a sedimentary component introduced into the mantle wedge when subduction began. A contribution of forearc crustal material into the mantle via subduction erosion was not totally ruled out by Mpodozis and Kay (1992). On this regard it is worth mentioning that Gerya and Meilick (2011) have recently developed a model for subduction zones in which they consider magmatic arc formation. Following that model, subducted trench sediments reach the magmagenic zone 25 to 30 my after the initiation of subduction, and may form what they describe as cold plumes. After Willner et al. (2012), the convergence in this segment of the Gondwana margin was initiated at some time between 343 and 310 Ma in agreement with the model. This sedimentary material, is partially melted to contribute to the arc magmas, and imposes the characteristics of recycled continental crust. The metasedimentary material can be exhausted if mass balance favors the subducted mass over the volume of sedimentary material in the trench, and thus either extinguishes the arc magmatism. Or, evolve to a mantle derived magma, as is observed with time in the Elqui section where the younger, metaluminous early Guanta type biotite-hornblende tonalites show a diminished crustal component with time (Mpodozis and Kay, 1992). However, a more conventional model is that mantle derived magmas are mixed and homogenized in the lower crust and/or contaminated in the upper crust during shallow pluton emplacement (Hildreth and Moorbath, 1988).

The zircon Hf–O isotopic dataset shows that the magmatic evolution from the early Permian to the late Permian–Triassic produced a sharp decrease in the involvement of crustal material during the genesis of the magmas and an increase in juvenile components. This agrees with the change to a more extensional regime that prevailed after the older components of the batholiths were uplifted and exhumed following the “San Rafael” event when, according to Mpodozis and Kay (1992) subduction ceased along the Pacific Gondwana margin. At that time large amounts of juvenile basaltic magmas appear to have been intruded. These would have melted the base of the crust, comprising the mafic roots of the former Early Permian arc, and evolved to produce the large volume of silicic magmas emplaced during the Late Permian and Triassic along most of the Frontal Cordillera in Chile and Argentina.

6.4. Regional correlations

The Chilean Frontal Cordillera batholiths form part of a long Late Paleozoic–Early Mesozoic magmatic belt that can be traced from Central Peru (Cordillera de Marañón) to La Pampa Province in Argentina. The northernmost outcrops of this semi -continuous magmatic belt have been recently studied by Mišković et al. (2009). On the basis of a large U–Pb age dataset, the Late Paleozoic magmatism in Peru started, as in the Elqui Limarí batholith, in the Carboniferous and lasted until the late Triassic with four main peaks of magmatism in the Mississippian (350–325 Ma), Late Pennsylvanian–Early Permian (315–285 Ma), Permian to Triassic (249–223 Ma) and Upper Triassic–Lower Jurassic (216–190 Ma). Whilst the two older episodes are formed by calc-alkaline rocks with elevated LILE/HFSE ratios typical of continental arc magmas, the Permian to Triassic and Triassic intrusives are S- to A-type granitoids emplaced when widespread crustal extension and thinning affected the western Gondwana margin (Miskovic and Schaltegger, 2009). Zircon Lu–Hf isotopic data suggest that the Carboniferous to early Permian arc intrusives include a large crustal component involved in the magmagenesis that, as in Central Chile, dramatically decreased during the Permian to Triassic (Miskovic and Schaltegger, 2009).

There is insufficient combined geochronological and geochemical data from northern Chile to allow for a precise comparison with Peru and the Chilean Frontal Cordillera, although U–Pb ages available from various sources range from 320 to 200 Ma, as in central Peru,. Moreover, no U–Pb zircon ages have been published for the Frontal Cordillera of San Juan-Mendoza, in Argentina. U–Pb zircon ages reported further south in the San Rafael block by Rocha-Campos et al. (2011) and Domeier et al. (2012) are mainly Permian (281–251 Ma). Nevertheless, U–Pb zircon ages recently published by Suárez et al. (2012) for the classical locality of Cordillera del Viento in Neuquén, south of San Rafael (Llambías et al., 2007) indicate a protracted history of magmatism with events dated at 328–325 Ma (Mississippian) 304 to 281 Ma (Pennsylvanian–early Permian) and 198–196 Ma (earliest Jurassic). Even if the Late Permian to Triassic episodes has not been recorded there, these events may be compared with those recorded in the Elqui–Limarí and Chollay batholiths and central Peru.

Pankhurst et al. (1996) and Parada et al. (2007) have suggested that the Chilean Frontal Cordillera batholiths initially formed a continuous belt with the Late Paleozoic Coastal Batholith of south Central Chile which were separated as a result of Meso-Cenozoic extension during later stages of the Andean Orogeny. However, recent data makes it difficult to support such proposal as, over a distance of 800 km, the Coastal Batholith has yielded numerous 320 to 300 Ma (Pennsylvanian) U–Pb zircon ages (Deckart et al., in press) which do not overlap with the available ages obtained for the plutons of the Frontal Cordillera batholiths. No Permian and Early Triassic granitoids intrude the main body of the Costal Batholith, although some small late Triassic–early Jurassic stocks of calc-alkaline to transitional A-type affinities, with U–Pb zircon ages from 225 to 197 Ma, are emplaced into its metamorphic envelope (Vásquez et al., 2011). The Pennsylvanian Coastal Batholith intrusives differ from the early Permian and early Triassic granitoids of the Elqui–Limarí and Chollay batholiths, respectively, in having zircons with higher $\delta^{18}O$ (6.4 to 8.6‰) and lower εHf (+1.67 to −5.64) values (Deckart et al., in press). Based on whole rock Nd–Sr–Pb isotopic compositions Lucassen et al. (2004) and Vásquez et al. (2011) have suggested that the mildly peraluminous rocks of the Coastal Batholith show contributions of a crustally-derived sediment source in the magmas, with a predominance of juvenile sources for the late Triassic–early Jurassic rocks.

7. Conclusions

The Frontal Cordillera batholiths in the Andes of north Central Chile (28–31°S) evolved from the Mississippian to the Late Triassic as a result of four discrete magmatic pulses: Mississippian (330–326 Ma), early Permian (301–284 Ma), late Permian–Middle Triassic (264–242 Ma) and Upper Triassic (225–215 Ma). The oldest ages obtained here are considered to represent magmatism associated with the onset of subduction along the South American section of the Gondwana margin, after collision of the Chilenia microplate.

The zircon O and Lu–Hf isotopic data for the Elqui batholith shows an evolution from crustally derived values for magmas during the Early Permian magmatic arc phase, to more mantle-like compositions during the Late Permian–Triassic when extensional conditions prevailed after an episode of exhumation and uplift. The chronology and geochemical signatures of the Elqui–Limarí and Chollay batholiths are comparable to those of the Late Paleozoic Early Mesozoic batholiths of central Peru and in part with the chronology of the magmatic events recorded at Cordillera del Viento in Neuquén, Argentina. However, the magmatic history of the Elqui–Limarí and Chollay batholiths differs from the evolution of the Coastal Batholith of Central Chile where a magmatic gap of nearly 100 Ma separates the emplacement of Pennsylvanian granitoids from younger, Late Triassic–Early Jurassic, intrusives.

Supplementary data to this article can be found online at http://dx.doi.org/10.1016/j.lithos.2013.10.018.

Acknowledgments

This research was funded by FONDECYT project 1095099. C. Maureira accompanied on one of the field trips. J. Vargas (Universidad de Chile) skillfully separated the zircons. P. Holden and L. Kinsley (ANU) are thanked for the assistance with the O and Hf isotopic data respectively. Revisions by Dr. Paulina Vásquez (Sernageomin, Chile) and Dr. David Chew (Trinity College, Ireland) greatly improved the original version.

References

Alasino, P.H., Dahlquist, J.A., Pankhurst, R.J., Galindo, C., Casquet, C., Rapela, C.W., Larrovere, M.A., Fanning, C.M., 2012. Early Carboniferous sub- to mid-alkaline magmatism in the Eastern Sierras Pampeanas, NW Argentina: A record of crustal growth by the incorporation of mantle-derived material in an extensional setting. Gondwana Research 22, 992–1008.

Álvarez, J., Mpodozis, C., Arriagada, C., Astini, R., Morata, D., Salazar, E., Valencia, V.A., Vervoort, J.D., 2011. Detrital zircons from late Paleozoic accretionary complexes in north-central Chile (28°–32°S): Possible fingerprints of the Chilenia terrane. Journal of South American Earth Sciences 32, 460–476.

Álvarez, J., Mpodozis, C., Blanco-Quintero, I.F., García-Casco, A., Morata, D., Arriagada, C., 2013. U/Pb geochronology and P-T-t path of the La Pampa Gneisses, implications for the evolution of the Chilenia Terrane and Permo-Triassic tectonics of North-Central Chile. Journal of South American Earth Sciences 47, 100–115.

Astini, R.A., Martina, F., Ezpeleta, M., Dávila, F.M., Cawood, P.A., 2009. Chronology from rifting to foreland basin in the Paganzo Basin (Argentina), and a reapprisal on the "Eo- and Neo Hercynian" tectonics along Western Gondwana. XII Congreso Geológico Chileno, Proceedings (CD ROM), Santiago, Chile.

Bahlburg, H., Hervé, F., 1997. Geodynamic evolution and tectonostratigraphic terranes of northwestern Argentina and northern Chile. Geological Society of America Bulletin 109 (7), 869–884.

Bahlburg, H., Vervoort, J.D., Du Frane, S.A., Bock, B., Augustsson, C., Reimann, C., 2009. Timing of crust formation and recycling in accretionary orogens: insights learned from the western margin of South America. Earth Science Reviews. http://dx.doi.org/10.1016/j.earscirev.2009.10.006.

Black, L.P., Kamo, S.L., Allen, C.M., Aleinikoff, J.N., Davis, D.W., Korsch, R.J., Foudoulis, C., 2003. TEMORA 1: a new zircon standard for Phanerozoic U-Pb geochronology. Chemical Geology 200, 155–170.

Bolhar, R., Weaver, S.D., Whitehouse, M.J., Palin, J.M., Woodhead, J.D., Cole, J.W., 2008. Sources and evolution of arc magmas inferred from coupled O and Hf isotope systematics of plutonic zircons from the Cretaceous Separation Point Suite (New Zealand). Earth and Planetary Earth Sciences Letters 268, 312–324.

Cawood, P.A., 2005. Terra Australis orogen: Rodinia breakup and development of the Pacific and Iapetus margins of Gondwana during the Neoproterozoic and Paleozoic. Earth Science Reviews 69, 249–279.

Chew, D.M., Schaltegger, U., Kosler, J., Whitehouse, M.J., Gutjahr, M., Spikings, R.A., Miskovic, A., 2007. U–Pb geochronologic evidence for the evolution of the Gondwanan margin of the north-central Andes. Geological Society of America Bulletin 119 (5/6), 697–711.

Coloma, F., Salazar, E., Creixell, C., 2012. Nuevos antecedentes acerca de la construcción de los plutones Pérmicos y Permo-Triásicos en el valle del río Tránsito, región de Atacama, Chile. XIII Congreso Geologico Chileno, Antofagasta, Actas electrónicas.

Dahlquist, J.A., Pankhurst, R.J., Gasching, R.M., Rapela, C.W., Casquet, C., Alasino, P.H., Galindo, C., Baldo, E.G., 2013. Hf and Nd isotopes in Early Ordovician to Early Carboniferous granites as monitors of crustal growth in the Proto-Andean margin of Gondwana. Gondwana Research 23 (4), 1617–1630.

Deckart, K., Hervé, F., Fanning, C.M., Ramírez, V., Calderón, M., Godoy, E., 2014. U-Pb geochronology and Hf-O isotopes of zircons from the Pennsylvanian Coastal Batholith, South-Central Chile. Andean Geology. http://dx.doi.org/10.5027/andgeoV41n1-a03 (in press).

Domeier, M., Van der Voo, R., Torsvik, T.H., 2012. Review Article: Paleomagnetism and Pangea: The Road to reconciliation. Tectonophysics 514–517, 14–43.

Gerya, T.V., Meilick, F.I., 2011. Geodynamic regimes of subduction under an active margin: effects of rheological weakening by fluids and melts. Journal of Metamorphic Geology 29, 7–31.

Gregori, D., Benedini, L., 2013. The Cordon del Portillo Permian magmatism, Mendoza, Argentina, plutonic and volcanic sequences at the western margin of Gondwana. Journal of South American Earth Sciences 42, 61–73.

Gregori, D.A., Greco, L.E., Llambías, E., 2003. El intrusivo López Lecube: Evidencias de magmatismo alcalino Gondwánico en el sector sudoeste de la provincia de Buenos Aires, Argentina. Revista de la Asociación Geológica Argentina 58, 176–186.

Grosse, P., Söllner, F., Baéz, M.A., Toselli, A.J., Rossi, J.N., de la Rosa, J.D., 2009. Lower Carboniferous post-orogenic granites in central-eastern Sierra de Velasco, Sierras Pampeanas, Argentina: U–Pb monazite geochronology and Sr–Nd isotopes. International Journal of Earth Science 98, 1001–1025.

Hildreth, W., Moorbath, S., 1988. Crustal contributions to arc magmatism in the Andes of Central Chile. Contributions to Mineralogy and Petrology 98, 455–489.

Ickert, R.B., Hiess, J., Williams, I.S., Holden, P., Ireland, T.R., Lanc, P., Schram, N., Foster, J.J., Clement, S.W., 2008. Determining high precision, in situ, oxygen isotope ratios with a SHRIMP II: analyses of MPI-DING silicate-glass reference materials and zircon from contrasting granites. Chemical Geology 257, 114–128.

Iizuka, T., Campbell, I.H., Allen, C.M., Gill, J.B., Maruyama, S., Makoka, F., 2013. Evolution of the African continental crust as recorded by U–Pb, Lu–Hf and O isotopes in detrital zircons from modern rivers. Geochimica et Cosmochimica Acta 107, 96–120.

IUGS (International Union of Geological Sciences), 2013. International Chronostratigraphic Chart, v 2013/01.

Kay, S.M., Ramos, V.A., Mpodozis, C., Sruoga, P., 1989. Late Paleozoic to Jurassic silicic magmatism at the Gondwana margin: analogy to middle Proterozoic in North America? Geology 17, 324–328.

Kleiman, L.E., Japas, M.S., 2009. The Choiyoi volcanic province at 34–36°S (San Rafael, Mendoza, Argentina): implications for the Late Paleozoic evolution of the southwestern margin of Gondwanana. Tectonophysics 473, 282–299.

Lambías, E.J., Sato, A.M., 1990. El batolito de Colanguil (29–31°S): estructuras y marco tectónico, Cordillera Frontal de Argentina. Revista Geologica de Chile 17 (1), 89–108.

Llambías, E.J., Sato, A.M., 1995. El batolito de Colangüil: transición entre orogénesis y anorogénesis. Revista de la Asociación Geológica Argentina 50, 111–131.

Llambías, E., Leanza, H., Carbone, O., 2007. Evolución tectono-magmática durante el Pérmico al Jurásico temprano en la Cordillera del Viento (37º05′/37°15′S): nuevas evidencias geológicas y geoquímicas del inicio de la cuenca neuquina. Revista de la Asociación Geológica Argentina 62, 217–235.

López Gamundi, O., 2006. Permian plate margin volcanism and tuffs in adjacent basins of west Gondwana: Age constraints and common characteristics. Journal of South American Earth Sciences 22, 227–238.

Lucassen, F., Trumbull, R., Franz, G., Creixell, C., Vásquez, P., Romer, R.L., Figueroa, O., 2004. Distinguishing crustal recycling and juvenile additions at active continental margins: the Paleozoic to recent compositional evolution of the Chilean Pacific margin (36–41°S). Journal of South American Earth Sciences 17, 103–119.

Martin, M.W., Clavero, J., Mpodozis, C., 1999. Late Palaeozoic to Early Jurassic tectonic development of the high Andean Principal Cordillera, El Indio region, Chile (29º–30ºS). Journal of South American Earth Sciences 12, 33–49.
Martina, F., Viramonte, J.M., Astini, R.A., Pimentel, M.M., Dantas, E., 2011. Mississippian volcanism in the south-central Andes: new U–Pb SHRIMP zircon geochronology and whole-rock geochemistry. Gondwana Research 19, 524–534.
Massonne, H.-J., Calderón, M., 2008. P–T evolution of metapelites of the Guarguaráz complex, Argentina: evidence for Devonian crustal thickening close to the western Gondwana margin. Revista Geologica de Chile 35, 215–231.
Miskovic, A., Schaltegger, U., 2009. Crustal growth along a non-collisional cratonic margin: a Lu–Hf isotopic survey of the Eastern Cordilleran granitoids of Perú. Earth and Planetary Science Letters 279, 303–315.
Mišković, A., Spikings, R.A., Chew, D.M., Košler, J., Ulianov, A., Schaltegger, U., 2009. Tectono-magmatic evolution of Western Amazonia: geochemical characterisation and zircon U–Pb geochronologic constraints from the Peruvian Eastern Cordilleran granitoids. Geological Society of America Bulletin 121 (9/10), 1298–1324.
Mpodozis, C., Cornejo, P., 1988. Hoja Pisco Elqui, Región de Coquimbo. Servicio Nacional de Geología y Minería. Carta Geológica de Chile. No 68 (1:250.000), 164 pp.
Mpodozis, C., Ramos, V., 1989. The Andes of Chile and Argentina. In: Ericksen, G.E., Cañas, M.T., Reinemund, J.A. (Eds.), Geology of the Andes and its relation to hydrocarbon and mineral resources. Circum-Pacific Councyl for Energy and Mineral Resources Earth-Science Series, vol. 11, pp. 59–90.
Mpodozis, C., Kay, S.M., 1990. Provincias magmáticas ácidas y evolución tectónica de Gondwana: Andes chilenos (28º–31°S). Revista Geologica de Chile 17 (2), 153–180.
Mpodozis, C., Kay, S.M., 1992. Late Paleozoic to Triassic evolution of the Gondwana margin: evidence from Chilean Frontal Cordilleran batholiths (28º–31ºS). Geological Society of America Bulletin 104 (8), 999–1014.
Mpodozis, C., Marinovic, C., Smoje, I., 1993. Estudio geológico- estructural de la Cordillera de Domeyko entre Sierra Limón Verde y Sierra Mariposas Región de Antofagasta. Servicio Nacional d Geologia y Mineria, Santiago, IR 93–04.
Munizaga, F., Maksaev, V., Fanning, C.M., Giglio, S., Yaxley, G., Tassinari, C.C.G., 2008. Late Paleozoice–Early Triassic magmatism on the western margin of Gondwana: Collahuasi area, Northern Chile. Gondwana Research 13, 407–427.
Murillo, I., Álvarez, J., Arriagada, C., Calderón, M., Charrier, R., 2012. Geología estructural del Valle de el Tránsito con énfasis en las Milonitas El Portillo, III Región, Chile. XIII Congreso Geologico Chileno, Antofagasta, Actas electrónicas.
Nasi, C., Mpodozis, C., Cornejo, P., Moscoso, R., Maksaev, V., 1985. El Batolito Elqui–Limari (Paleozoico Superior-Triásico): Características petrográficas, geoquímicas y significado tectónico. Revista Geologica de Chile 24–25, 77–111.
Nasi, C., Moscoso, R., Maksaev, V., 1990. Hoja Guanta, Región de Coquimbo. Servicio Nacional de Geología y Minería. Carta Geológica de Chile Nº 67 (1:250.000), 141 pp.
Pankhurst, R.J., Millar, I.L., Hervé, F., 1996. A Permo-Carboniferous U–Pb age for part of the Guanta unit of the Elqui–Limarí batholith at Rio del Tránsito, Northern Chile. Revista Geologica de Chile 23 (2), 35–47.
Parada, M.A., 1988. Pre-Andean peraluminous and metaluminous leucogranitoid suites in the high Andes of Central Chile. Journal of South American Earth Sciences 1, 211–221.
Parada, M.A., Munizaga, F., Kawashita, K., 1981. Edades Rb–Sr del batolito compuesto de los ríos Elqui–Limari a la latitud 30°S. Revista Geologica de Chile 13–14, 87–93.
Parada, M.A., López-Escobar, L., Oliveros, V., Fuentes, F., Morata, D., Calderón, M., Aguirre, L., Féraud, G., Espinoza, F., Moreno, H., Figueroa, O., Muñoz Ravo, J., Troncoso Vásquez, R., Stern, C.R., 2007. Andean magmatism. In: Moreno, T., Gibson, W. (Eds.), The Geology of Chile. The Geological Society, London, Special Publication, 4, pp. 115–146.
Pineda, G., Calderón, M., 2008. Geología del área Monte Patria-El Maqui, región de Coquimbo, Escala 1:100.000. SERNAGEOMIN: 44 h. Santiago. (Carta Geológica de Chile, Serie Geología Básica, n.116).
Pitcher, W.S., Atherthon, M.P., Cobbing, J., Beckinsale, R.D. (Eds.), 1985. Magmatism at a Plate Edge: The Peruvian Andes. Blackie Halstead Press, Glasgow.
Ramos, V.A., Jordan, T.E., Allmendinger, R.W., Mpodozis, C., Kay, S.M., Cortés, J., Palma, M., 1986. Paleozoic terranes of the central Argentine Chilean Andes. Tectonics 5 (6), 855–880.
Reutter, K., 1974. Entwicklung und Bauplan der chilenischen Hochkordillere im Bereich 29º südlicher Breite. Neues Jahrbuch für Geologie und Paläontologie 146 (2), 153–178.
Ribba, L., Mpodozis, C., Hervé, F., Nasi, C., Moscoso, R., 1988. El basamento del valle del Tránsito, Cordillera de Vallenar: eventos magmáticos y metamórficos y su relación con la evolución de los Andes chileno–argentinos. Revista Geologica de Chile 15, 126–149.
Rocha-Campos, A.C., Basei, M.A., Nutman, A.P., Kleiman, Laura E., Varela, R., Llambias, E., Canile, F.M., da Rosa, O.C.R., 2011. 30 million years of Permian volcanism recorded in the Choiyoi igneous province (W Argentina) and their source for younger ash fall deposits in the Paraná Basin: SHRIMP U–Pb zircon geochronology evidence. Gondwana Research 19, 509–523.
Salazar, E., Arriagada, C., Mpodozis, C., Martínez, F., Peña, M., Álvarez, J., 2009. Análisis Estructural del Oroclino de Vallenar: Primeros Resultados. 12th Congreso Geológico Chileno Abstract S9_026, Santiago.
SERNAGEOMIN, 2003. Mapa Geológico de Chile: version digital. Publicación geológica digital, No. 4, 2003. CDROM, versión 1.0, 2003. Base Geológica escala 1:1.000.000. Gobierno de Chile, Servicio Nacional de Geología y Minería, Subdirección Nacional de Geología.
Suárez, M., Fanning, C.M., Etchart, H., De La Cruz, R., 2012. New Carboniferous to Toarcian U–Pb SHRIMP ages from Cordillera del Viento, Neuquén, Argentina. XIII Congreso Geologico Chileno, Antofagasta, Actas electrónicas.
Valley, J.W., Lackey, J.S., Cavosie, A.J., Clechenko, C.C., Spicuzza, M.J., Basei, M.A.S., Bindeman, I.N., Ferreira, V.P., Sial, A.N., King, E.M., Peck, W.H., Sinha, A.K., Wei, C.S., 2005. 4.4 billion years of crustal maturation: oxygen isotope ratios of magmatic zircon. Contributions to Mineralogy and Petrology 150, 561–580.
Vásquez, P., Glodny, J., Franz, G., Frei, D., Romer, R.L., 2011. Early Mesozoic Plutonism of the Cordillera de la Costa (34–37°S), Chile: constraints on the onset of the Andean Orogeny. The Journal of Geology 119 (2), 159–184.
Williams, I.S., 1998. U–Th–Pb geochronology by ion microprobe. In: McKibben, M.A., Shanks, W.C., Ridley, W.I. (Eds.), Applications of Microanalytical Techniques to Understanding Mineralizing Processes. Reviews in Economic Geology, 7, pp. 1–35.
Willner, A., Gerdes, A., Massonne, H.J., Schmidt, A., Sudo, M., Thomson, S., Vujovich, G., 2011. The geodynamics of collision of a microplate (Chilenia) in Devonian times deduced by the pressure–temperature–time evolution within part of a collisional belt (Guarguaraz Complex, W-Argentina). Contributions to Mineralogy and Petrology 162, 303–327.
Willner, A., Massonne, H.-J., Ring, U., Sudo, M., Thomson, S.N., 2012. P–T evolution and timing of a late Palaeozoic fore-arc system and its heterogeneous Mesozoic overprint in north-central Chile (latitudes 31–32°S). Geological Magazine 149, 177–207.
Woodhead, J., Hergt, J., 2005. A preliminary appraisal of seven natural zircon reference materials for in situ Hf isotope determination. Geostandards and Geoanalytical Research 29, 183–195.